COMPUTATIONAL ANALYSIS OF NANOSTRUCTURES FORMED IN MOLTEN SALT NANOFLUIDS

by

VIDULA B PAWAR

Presented to the Faculty of the Graduate School of

The University of Texas at Arlington in Fulfillment

of the Requirements

for the Degree of

MASTERS OF SCIENCE IN MECHANICAL ENGINEERING

THE UNIVERSITY OF TEXAS AT ARLINGTON

December 2014

Acknowledgements

I would first and foremost extent my gratitude towards my adviser, Dr. Donghyun Shin for his timely support, advice and encouragement in this entire research as well as Master's journey. This dissertation wouldn't have been possible without his guidance and motivation throughout.

Next, I would like to express thanks to my committee members, Dr. Dereje Agonafer and Dr. Adnan Ashfaq, for taking time out from their busy schedules and accept my request to serve as my committee members. Their advice on my research has proved to be enlightening for me. Thanks to Ms. Debi Barton for her welcoming and helping nature with all the administrative work which made this journey on alien land so smooth and warm.

I am also grateful to my lab member, Mr.Hani Tiznobaik, Mr.Joohyun Seo, Mr.Sumeet Changla, and Mr.Sriram Sambasivam for their constant support and help whenever requested. I am in debt with my UTA family; Chinmay, Ameya, Dr.Prasad, Shalini, Swati, Rashmi, Shweta, Kruti for their support throughout. I am obliged to my dear friend Kiran, for his patience to listen out to me whenever needed along with Neha, Richa, Preeti and Ishan. Also, Heena Ma'am, my teacher for life.

Finally, last but the most important, my parents and my dear brother; without whom this achievement would have been impossible. This is wholly and solely dedicated to them.

.

November 20, 2014

Abstract

COMPUTATIONAL ANALYSIS OF NANOSTRUCTURES FORMED IN MOLTEN SALT NANOFLUIDS

Vidula Pawar, M.S.

The University of Texas at Arlington, 2014

Supervising Professor: Donghyun Shin

Meeting the continuously increasing demand of 'clean' energy is the biggest challenge of the energy research field. Amongst the many renewable sources of energy, energy from the Sun is one of the biggest sources in the form of light and heat. Photovoltaic cells and concentrated solar power are few of the solar energy harnessing technologies. Photovoltaic cells use semiconductor materials to directly convert energy from sun into electricity. CSP uses a combination of solar receivers (mirrors or lenses) to concentrate the solar thermal energy which is further converted into electricity using the common thermodynamic cycle. One of the Photovoltaic (PV) technology's disadvantages over CSP is that it delivers power only in direct sunlight and it cannot store excess amounts of produced energy for later use. This is overcome by CSP. Thermal energy storage (TES) devices are used in CSP which store large amount of thermal energy for later use. TES use organic materials like paraffin wax, synthetic oils etc. as their heat transfer fluids (HTF).

One of the drawbacks of CSP technology is the limiting operating temperatures of HTF (up to 400 ^{o}C), which affects the theoretical thermal efficiency. Increasing this operating temperature up to 560 ^{o}C, which is the creeping temperature of stainless steel, can enhance the efficiency (from 54% to 63%). Hence, the uses of molten salts, which are thermally stable up to 600 ^{o}C, have been proposed to use as TES. With advantages of high operating temperature, low cost and environmentally safe these salts have

disadvantage of poor thermo-physical properties like low specific heat capacity and thermal conductivity.

A lot of experimental results of enhancements in the thermo-physical properties of molten-salt embedded with nanofluids have been reported. Nanofluids are solvents doped with nanoparticles. These reports suggest formation of nanostructures with liquid layer separations in the base salts as possible cause of enhancements. But there has been very limited computational analysis study to support these findings.

Tiznobaik et al saw nanostructure formed near nanoparticles and concluded it to be the primary cause for the enhanced specific heat capacity in carbonate nanofluids, (Li2CO3-K2CO3/SiO2). The formation of nanostructure was reasoned with dense layers and concentration gradient seen within the surrounding molten salt mixture. In this study an attempt has been made to elucidate and support this finding using computational analysis. Molecular Dynamic simulations have been performed using LAMMPS to analyze the cause of nanostructure formations. For the simulation, a periodic box of Li2CO3-K2CO3 (62:38) and a SiO2 nanocluster was made in Material Studio. After lot of initializations, a stable system was achieved and analysis showed concentration gradient around the nanocluster.

Same analysis will help to prove the theory of concentration gradient in other combination of salts and nanomaterials. This will also act as a base for finding the thermo-physical properties like heat capacity, thermal conductivity, density etc. of such salts to further validate the experimental results showing their enhancements.

Table of Contents

List of Illustrations

List of Tables

Chapter 1

Introduction

Solar Technology

Solar energy is one of the cleanest renewable energy resources that does not compromise or add to the global warming. The sun radiates more energy in one second then people have used since beginning of time. It is often termed as “alternative energy” to fossil fuel energy [1]. The growing scarcity of fossil fuels has raised global interest in the harnessing of solar energy [2-6]. With the ever increasing global warming issues contrary to ever increasing energy demand, making cheap and abundant energy with minimal environmental and ecological hazards available is one of important challenges faced today by the energy research industry. The sun provides us with 120,000 Tera watts of energy per hour [7]. Sun being the biggest source of everlasting thermal energy, power from sun has a great future potential. But at present it covers merely 0.05% of the total primary energy global supply. According to the 2010 BP Statistical Energy Survey, the world cumulative installed solar energy capacity was 22928.9MW in 2009, a change of 46.9% compared to 2008 [20].The reason is the difficulty in harnessing solar energy at economical rate with high efficiency. The other difficulty in using this thermal energy is that sunlight is available for just limited amount of time in a day which brings out the challenge of storing this energy for later times of the day.

Photovoltaic cells and concentrated solar power are few of the solar energy harnessing technologies. Photovoltaic cells use semiconductor materials to directly convert energy from sun into electricity. Photovoltaic cell technology first emerged as the best solar energy harnessing technology. But considering the requirement of use of energy for the time of the day when light is not available, the technology of concentrated solar power (CSP) emerged. CSP uses a combination of solar receivers (mirrors or

lenses) to concentrate the solar thermal energy which is further converted into electricity using the common thermodynamic cycle. As mentioned earlier, Photovoltaic (PV) technology has a disadvantage over CSP of delivering power only in direct sunlight and it cannot store excess amounts of produced energy for later use. CSP works irrespective of availability of direct sunlight.

Concentrated Solar Power

Concentrated solar power uses the simple technology of concentrating a large area of sunlight onto a small area using combination of mirrors or lenses. This concentrated light is then converted to heat using solar receivers. This heat energy drives a heat engine (usually a steam turbine) connected to an electrical power generator which finally generates electricity [8]. The heat energy is transferred to Thermal energy storage (TES) devices using heat transfer fluids (HTF). This TES are used in CSP to store large amount of thermal energy from the sun during day which is available for later use. Organic materials like paraffin wax, synthetic oils etc. as are most commonly used heat transfer fluids (HTF).

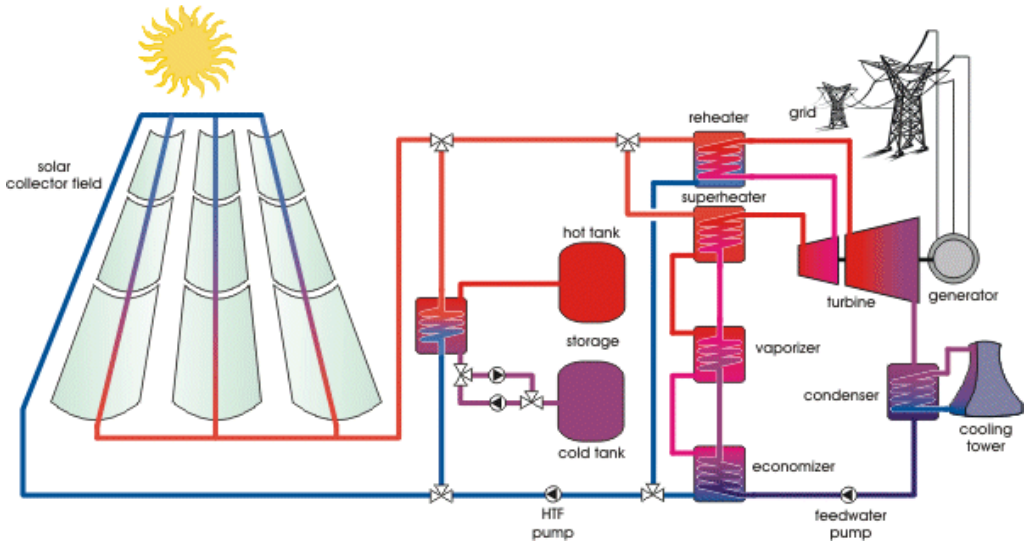

Figure 1 Block diagram of CSP [9]

The different solar receivers available are parabolic trough system, power tower systems and Concentrating dish receivers. In parabolic trough, the light energy is concentrated over a tube placed at the center of the parabolic shaped mirror where as in power tower system; it is concentrated on a single point located on a tower using combination of multiple mirrors. Concentrating dish works on the same principle as parabolic trough but for a small scale energy production using sterling engines.

As mentioned earlier, CSP has the privilege to store the sun's energy and make use of the stored heat to generate electricity in the later stages of the day. The potential to store energy cost-effectively and to deliver this as electricity when needed is a huge task and also the greatest strength of the CSP compared to other forms of energy harvesting [10].

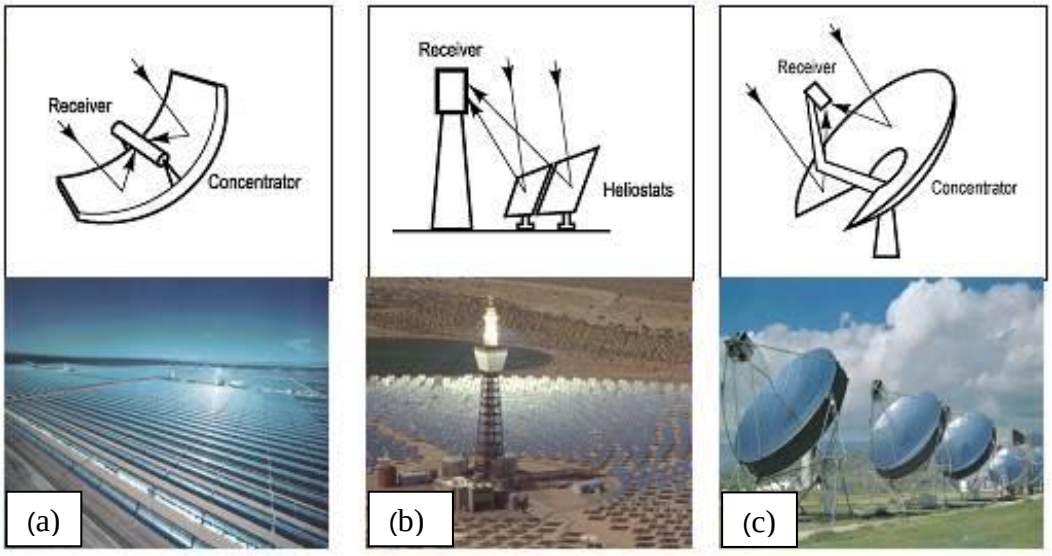

Figure 2 Different receivers-(a) Parabolic trough systems (b) Power tower systems (c) Concentrating dish systems

In any production power plants efficiency and cost are two important factors. The solar thermal power plants are heavily dependent on the high temperature of thermal storage units for continuous operation. Conventional TES materials are organic-based

(e.g., paraffin wax, fatty acid, mineral oil, etc.), which are thermally stable only up to 400 ^{o}C. This limits the operating temperature of the system to around 400 ^{o}C [11]. Increasing the operating temperature from 300–400 ^{o}C to 560 ^{o}C, which is the creep starting temperature of stainless steel, can significantly enhance the theoretical thermodynamic efficiency (the Carnot efficiency can increase from 50% to 65%). However, very few materials are compatible for the high temperature applications. [12]. Hence, the use of molten salts (e.g., alkali nitrate salts, alkali carbonate salts, etc.), which are thermally stable up to 600 ^{o}C, have been recently proposed to use as HTF [13]. This HTF carries the heat to inside a boiler or to a storage area which is known as the thermal-energy storage (TES) [14]. TES are the one which act a thermal source tank which store the heat energy collected from the sun and deliver it at the later parts day when the sunlight is not available or when the demand is at peak. The TES aids as a direct supplement to the existing electricity conversion systems, which are usually rankine cycle turbines. Hence, these systems have greatest advantage of being applicable in most power generating plants. TES prevails to be cost-effective as it integrates with any power generating plant removing the extra charges for storage [15, 16]. The heat storage capacity of TES can help produce electricity up to 7.5 hours without sunlight. Using thermally stable material also amounts to reduction in material costs.

With multiple advantages of the molten salt, it sounds like a perfect HTF/TES. But like everything else, it also has its set of disadvantages. Typical molten salts have very poor thermo-physical properties, especially specific heat capacity. (cp is less than 2 kJ/kg _C [17,18]). To tackle this, doping the molten salt with nanoparticles of silica (SiO2), alumina (Al2O3), Titania (TiO2), Siliver (Ag), Gold (Au), Carbon Nanotubes etc. was proposed. There have been reports in the literature for significant enhancement in thermal conductivity due to this kind of doping [19-23].

Molten Salt and Nanofluids

Molten salts are inorganic salts which are in solid state at standard temperature and pressure (STP) but they enter the liquid phase at elevated temperature application. Their features being denser compared organic salts with high thermal stability, low vapor pressure, abundance, cheap but low specific heat capacity. Different molten salts are binary, ternary, quaternary combinations of nitrates, chlorides, sulphates, carbonates etc. in various ratios.

Nanofluids are nano sized particle dispersions in a liquid (In this study, molten salts) are termed as nanofluids [19]. Different Nanofluids are as mentioned previously, silica (SiO_2), alumina (Al_2O_3), Titania (TiO_2), Siliver (Ag), Gold (Au), Carbon Nanotubes. Due to the very large specific surface area of nanoparticles, the effect of surface charge of nanoparticles is significantly high as compared to the micro-scaled or high-scaled particles This result enhances the stability of the resulting nanoparticle/liquid mixture [12].

Chapter 2

Motivation and Objective

Motivation

With different proposals there have been many studies reported in enhancements of thermo-physical properties, especially specific heat capacity which highly affect the efficiency and cost of CSP. Table 1 account to few such reports.

Table 1 Reports for enhancements in specific heat capacity of molten salt nanofluids

Author	Nanoparticle/Base fluid	Concentration	Enhancement
Tiznobaik[12]	SiO2/Li2CO3-K2CO3	1.0 wt.%	25% in Cp
Dudda [25]	SiO2/NaNO3-KNO3	1.0 wt.%	27% in Cp
Shin [26]	SiO2/Li2CO3-K2CO3	1.0 wt.%	26% in Cp
Shin [27]	CNT/Li2CO3-K2CO3	0.5 wt.%	18% in Cp
Andreu-Cabedo, Patricia, [28]	SiO2/NaNO3-KNO3	1.0 wt.%	25% in Cp

The next step was to find the cause of such enhancements. For this purpose, the samples for the aforementioned Nanoparticle/Base fluids were studied more in details. The electron microscopy analyses of the experimental samples of eutectic salt nanofluids have shown formation of the micron-scale substructures. These special structures were observed to surround the nanoparticles and were termed as nanostructures. Fig. 3 is a schematic referring to the formation of nanostructures.

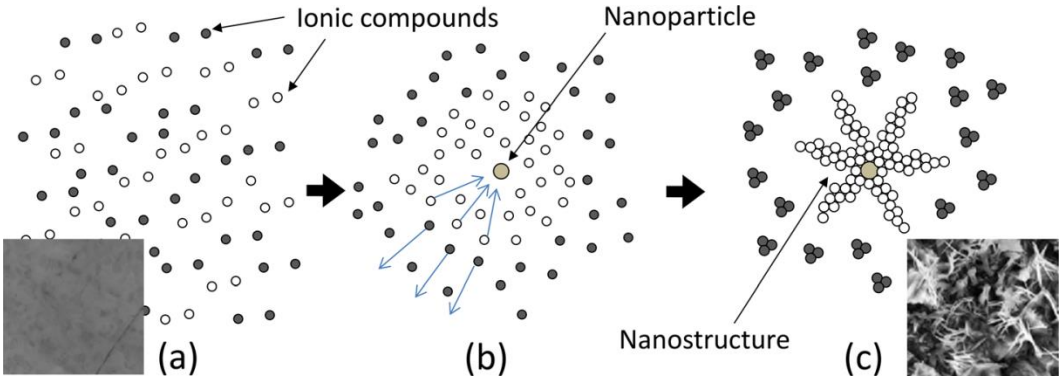

Figure 3 (a) Homogeneously dispersed ionic compound A (bright) and ionic compound B (dark). (b) When a nanoparticle is loaded, A is more attracted than B due to the difference in electrostatic interactions. A moves closer to and B moves away from the nanoparticle. (c) A portion of ionic compound A near the nanoparticle starts to crystallize and forms a fractal-like fluid nanostructure [29].

One such study report was by Tiznobaik et al where they investigated the specific heat capacity mechanism for a mixture of molten salt eutectic, lithium carbonate and potassium carbonate (62:38, molar ratio) doped with silicon-dioxide nanoparticles for high temperature applications to explain the specific heat capacity enhancement of the nanofluids. The differential scanning calorimeter was used to measure the specific heat capacity of the molten salt eutectic and nanomaterials [12]. These samples were further observed under SEM to study the changes in the structure and analyze the cause in the effects. From these images needle-like structures were observed all over the nanomaterials [Fig 4] as compared to the pure eutectics [Fig 5].They concluded that these structures are the cause for the enhancements in the thermo-physical properties.

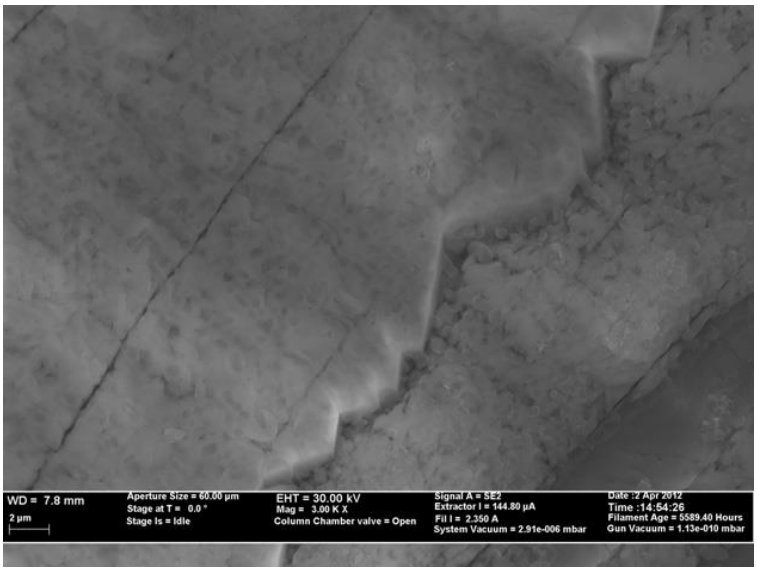

Figure 4 Scanning electron micrograph (SEM) of pure eutectic mixture after testing [12]

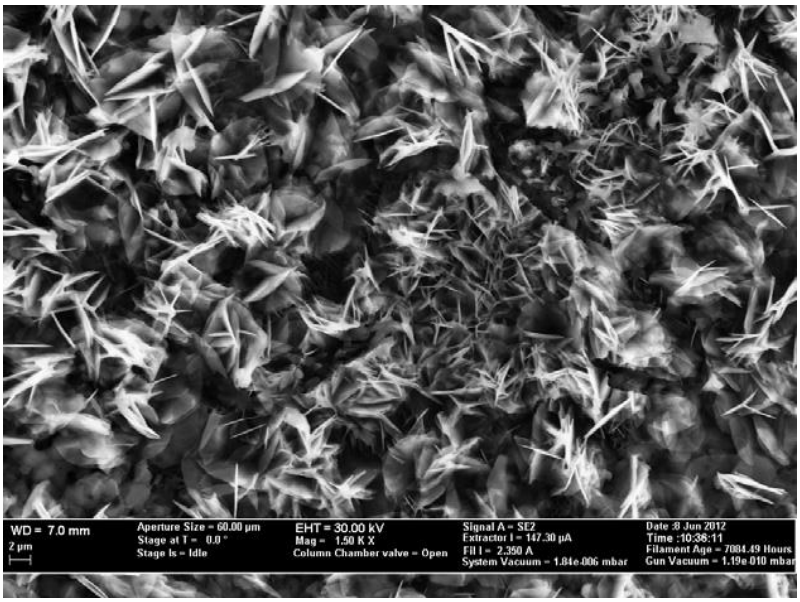

Figure 5 Scanning electron micrograph (SEM) of nanomaterial (30 nm) after testing [12]

Special needle-like structures are formed all over the nanomaterials. These structures are expected to have an exceptionally large specific surface area compared with the bulk eutectic material

It is a known phenomenon that liquid molecules tend to form a semi-solid layer on a solid surface. Similarly in molten salt eutectic, when nanoparticles are mixed, the molten salt molecules tend to form a semi-solid layer on the surface of the nanoparticle. In the molten salt carbonate eutectic (Li2-CO3 and K2CO3); it was proposed that there should be a concentration gradient of the mixture on the nanoparticle surface due to thermophoresis effect. This can cause a different molar composition of the mixture at the layering than the original composition of 62:38 and this induce further growth of layering to be the needle-like structure as seen in Fig.4.b The change in composition cab be analyzed by observing presence of dense spots in the samples. In Fig. 5 shows the backscattered electron micrograph that the needle-like structures are brighter than the bulk molten salt eutectic. The bright spots, as said earlier, indicate the structure has different molar composition from the bulk composition. The needle-like structures seen have very large specific surface areas as nanoparticles do adding to the effect of surface energy on the effective specific heat capacity. This contributes to the enhanced specific heat capacity of the nanomaterials as proposed by Tiznobaik et al.

Similar studies have been reported in the molten salt application area which study and analyze effects of adding nanoparticles. A lot of similar experimental analysis is available to show how the formation of nanostructures in the base salts affects the thermo-physical properties of molten salts. For experimental validation, support either from analytical or simulations is always considered. But for study of molten salts, there has been very limited simulations done to support for validations of such reports.

Considering an aim to perform computational analysis for carbonate salts, with literature survey one report of Li2CO3-K2CO3/CNT was found. The analysis reported the compressed (dense layer) formation around nanostructure, liquid layer separations and

also density value for the molten salt nanofluid. Molecular dynamic simulations were performed using LJ parameters mentioned in table 2.

Table 2 LJ parameters for Li2CO3-K2CO3/CNT [24]

Interactions	ε(kcal/mol)	σ[A]	Charge
C-C	0.055	3.617	1.54
O-O	0.228	2.88	-1.18
Li-Li	4.735	2.839	+1.00
K-K	5.451	3.197	+1.00
C-C (CNT)	0.055	3.412	0.00

The results obtained were as shown in the Figures 6 and 7.

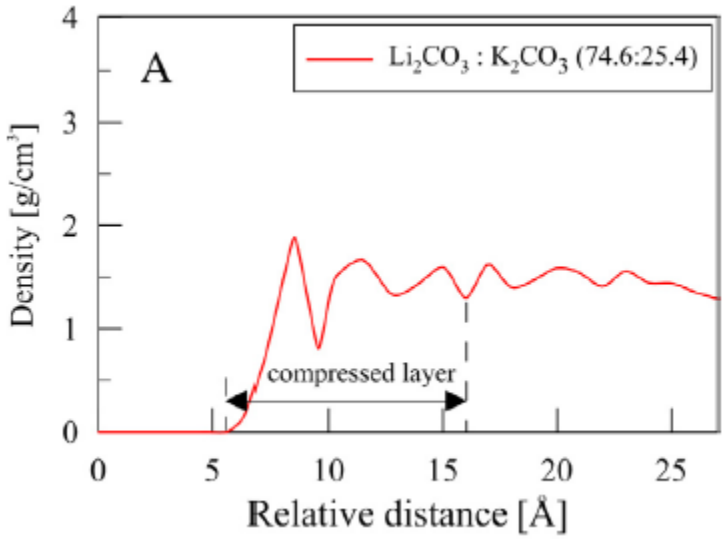

Figure 6 Density simulation plots for Li2CO3-K2CO3 (76.6:25.4) [24]

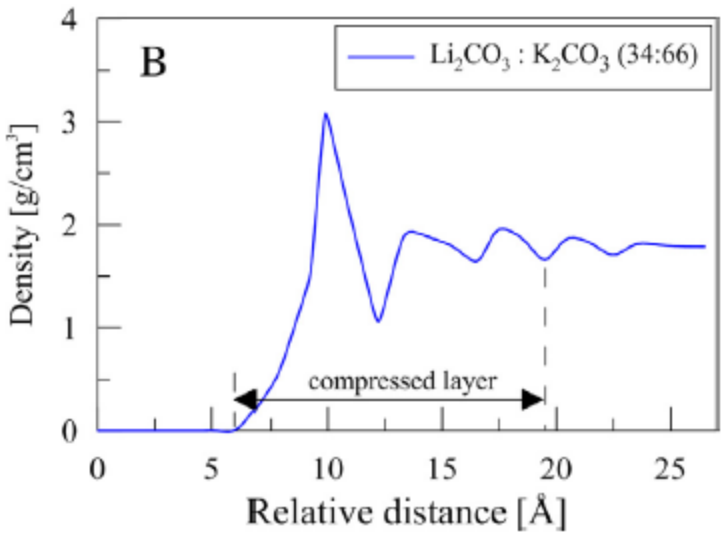

Figure 7 Density simulation plots for Li2CO3-K2CO3 (34:66) [24]

The density values obtained from this simulation were low as compared to the literature value of 1.9790825 kg/cm3. This was the next motivation to carry out the computational analysis with an aim to reduce this error.

This study is at a thermal study at nanoscale. At this scale, the usual thermal behaviors due to surface and environment interactions change. One of such interaction is the interfacial thermal resistance at the interface of nanoparticles and the molten salt. Measuring this property with experiments is extremely difficult and hence, in such cases, computational simulations are useful. This is the third motivation of this study.

Objective

The objectives thus were:

- Design and Simulate the SiO2/Li2CO3-K2CO3 system
    - To Compare density simulation results with existing simulation results
    - Improve the parameters
    - Study the cause of nanostructure formations.
    - Analyze the simulations for concentration gradients and liquid layer separations
- Study the Interfacial Thermal resistance at the interface of nanoparticle and the molten salt.

Chapter 3

Computational Analysis

Background

Computer (computational) simulations are simulations developed to replicate the behavior of real life, analytical and experimental models. They are a major part of mathematical modeling of many systems in various fields like Biology, Physics, Astrophysics, Chemistry, Engineering etc. They are useful when the traditional paper-and-pencil mathematical modeling fails. Sometimes achieving the required conditions in actual experiments is complex. For example, nuclear reactions, shock wave, high temperature plasma, cancer cells etc. Along with complexity, experiments with real life systems sometimes consume lot of time and the repeatability of the results can be unreliable. In all such situations, computer simulations help to reproduce better systems comparatively consuming less time. It is majorly used to validate the analytical and experimental findings in most of the areas. It acts like a bridge between models and theoretical predictions on one hand, and between models and experimental results on the other hands. [1] This dual role is best illustrated in the flow diagram below in Fig 8.

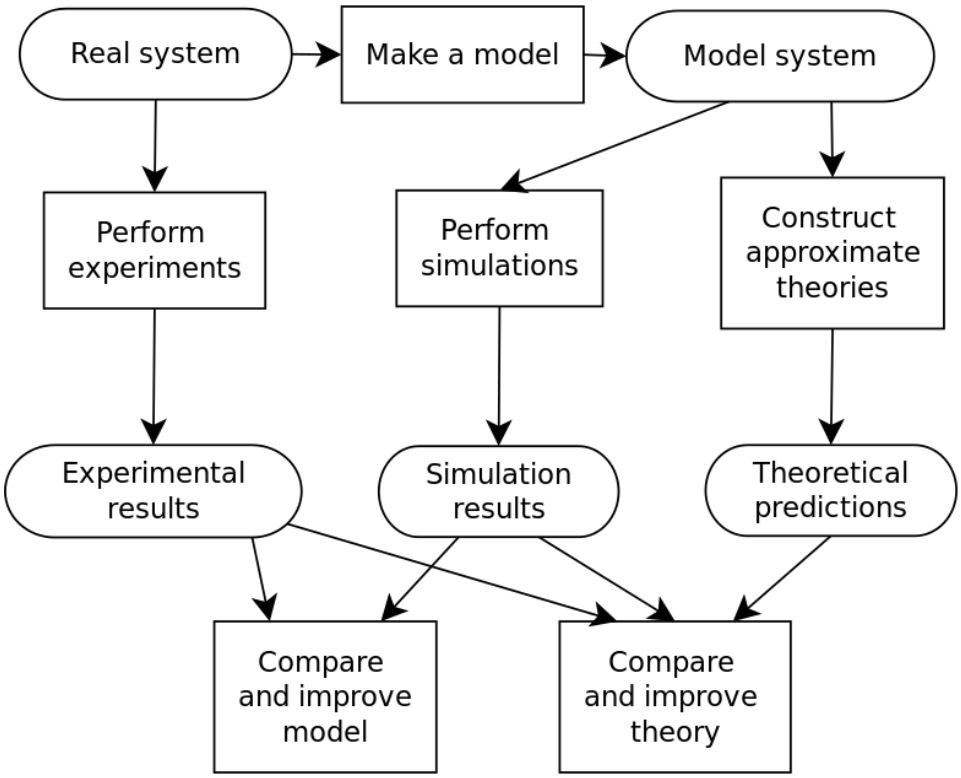

Figure 8 Schematic of computational analysis usefulness [30].

“Molecular Simulation" is a statistical tool to model or reproduce the behavior of molecules for a real life system. They provide exact solutions for the problems involving models based on statistical mechanics. Their results depend solely on the nature of the theoretical method. In molecular simulations the atomic system evolves in spatial and/or temporal domain in accordance with the extensive calculations of intermolecular energies. This is also the fundamental difference between the molecular simulations and the other computational methods.

There are two main types of molecular simulations:

Monte Carlo (MC) simulations

Molecular Dynamics (MD) simulations

There are other simulations where features of these two are used in combinations. They are called as Hybrid molecular simulations.

Monte Carlo simulations was developed and first used by von Neumann, Ulam and Metropolis to study the diffusion of neutrons in fissionable material. These simulations were named so because of the used of 'random numbers' in the calculations. It is developed as a stochastic method that relies on probability and random selections. It is a problem solving technique which approximates the probability of various certain outputs after multiple trial runs which use random variables. For these simulations, initial domain of variables is defined and by further by adding, removing, exchanging or displacing molecules a new trial configuration is generated. This is then evaluated against an acceptance criterion. At last, the configuration is either accepted or rejected. The acceptance criteria are based on the change in energy calculations and/or other properties of the system. Not all states contribute to the configurational properties. But states making significant contributions are sampled by generating Markov chains.

Molecular dynamic simulations involve calculation of time dependent behavior of a molecular system. It involves solving the various Newton's equations of motions for each atom and/or molecule of a system. The atoms and molecules interact for a period of time, giving an output view of motions. The trajectories of motion are determined by numerical solutions of Newton's equations of motion and the forces of interaction and potential energy between molecules and atoms are defined by molecular mechanics force fields. This method was developed by Alder and Wainwright in late 50s and Rahman in 60s. This method is frequently used in biological field to study and analyze complex structures like proteins.

Both of these methods have their own pros and cons depending majorly on the application. MC simulations are time independent defining the state of the system at one

particular time as compared to MD where the simulations are analyzed at various time steps. As MD involves solving of equation of motions at various time steps its computational cost is comparatively more. If other factors like rate of sample rejection are considered and are increased, the computational cost might increase. MC simulations work well for liquids with moderate density, systems of strongly coupled solids and cellular structures. MD simulations are suitable for liquids with high density, gaseous systems at high pressures and temperatures. Also, for system with dynamic properties like rheological properties, transport coefficients etc.

Molecular Dynamic Simulations

The behavior of atoms and molecules in all the systems are well defined by the classical equation of motions and in most condition, Newton's law of motion. MD is a very powerful computation method which works on the same principle to study the dynamic nature of various solid, liquid and gaseous systems. This method numerically integrates the Newton's equation of motion for the system atoms and molecules. The output is a temporal evolution of co-ordinates and momenta of the atoms and molecules. The value is discrete and at each time step represents the microstate at the particular ensemble. This way the classical mechanics equations are used to evaluate the various system properties.

As mentioned, MD is based on Newton's equation of motion which for an atom *i* can be expressed as:

$$F_i(t) = m\ddot{r}_i(t) \tag{2.1}$$

Hence, for a system constituted with *N* atoms having mass m_i, for each atom *i*; F_i is the force acting upon it, due to the interactions with other atoms. Therefore, as against Monte Carlo simulations, molecular dynamics is a deterministic technique when initial set of positions and velocities are known. It gives subsequent time evolution of the system. If

we imagine this, we can picture atoms willing to “move” into the computer, bumping into each other, wandering around (if the system is fluid), oscillating in waves in concert with their neighbors, perhaps evaporating away from the system if there is a free surface, and so on, in a way pretty similar to what atoms in a real substance would do. [3]

For this system with *N* atoms, the intermolecular potential energy is defined by $E(r^N)$, where $r^N = r_1; r_2; r_3; \ldots\ldots ; r_{N;}$ center of mass of atoms. This intermolecular potential energy is defined by a set of various parameters which are termed nothing but as force fields.

Considering no dissipative force acts among the atoms, the force acting on atom *i* can be given by the potential function as,

$$F_i(t) = -\frac{\partial E(rN)}{\partial r_i} \qquad (2.2)$$

Combining the above two equations (2.1) and (2.2),

$$F_i(t) = m\ddot{r}_i(t) = -\frac{\partial E(rN)}{\partial r_i} \qquad (2.3)$$

The first integration of this equation gives the atomic momentum at next time step and the second integration gives atomic positions. If further integrations are carried out we can obtain position trajectories which can be used to get the macroscopic properties of the system using the classical mechanics equations [31]. Due to the complexity of integration of equation of motions for atomic systems, numerical integrations are used. For this, among the many available schemes, verlet algorithm and Gear Predictor-corrector are most commonly used.

Molecular dynamic simulations can be best described using following features. They are the defining parameters for a simulation to be carried out for a particular system.

I. Boundary Conditions

Simulating a whole system means a high computational cost with a long time to complete it. Hence, to prevent this, the system is divided in small discrete sections. These small systems are then used to perform simulations. When the big system is divided into small discrete systems, the edge atoms have few atoms to interact. They are the once whose interactions introduce the surface effect which ultimately affect the bulk properties of the system. Hence, they might cause negative effect in the simulations. To avoid these surface effects, the entire system must be simulated. But as mentioned before, it will involve huge computational complexity, cost and time. The solution to this is considering the boundary conditions for the system to be periodic. The pictorial representation of this explanation is well described by the fig. 9 below.

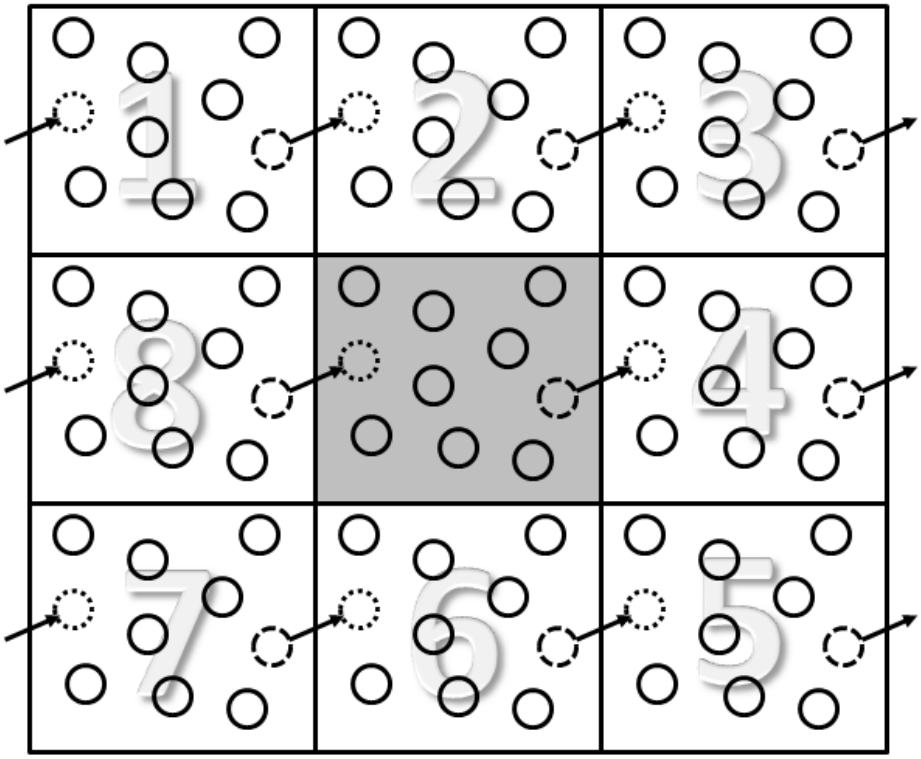

Figure 9 Periodic Boundary Conditions [31]

Further explaining PBC in a 2-D system, the small discrete section of the system considered is replicated infinitely in space lattice. When a simulation runs, one particle like ion/atom/molecule leaves, a same kind of particle enters from the opposite end. This way for the original simulation box at the center, if a particle leaves the right edge of the box, its image enters this box simultaneously. This makes the center box devoid of all boundaries solving the problem of surface effects mentioned earlier.

Periodic Boundary conditions also helps in building the neighboring lists. This list consists of particles positioned within the cut-off distance of each particle. This involves the non-bonded interactions. Particles at the center and around will have neighboring atoms within the same box. But for the particles at the edge, they have no neighboring atoms to interact if periodic boundary conditions are not applied.

II. Force Field

Force field; also termed as potential energy functions; are nothing but parameters obtained from mathematical equations. They define the interaction between the particles of the system. According to Brenner [32], an effective force field should possess following four critical properties,

- Flexibility: A potential function must be flexible enough to accommodate a wide range of fitting data derived from experiments and ab-initio calculations.
- Accuracy: A potential function should be able to accurately reproduce an appropriate fitting data base.
- Transferability: A potential function should be able to describe at least qualitatively, if not with quantitative accuracy, structures not included in a fitting data base.

- Computational efficiency: The function evaluation should be computationally efficient depending upon the system size and time scales of interest as well as the available computer resources.

There are a large number of force fields available in the literature, which can be broadly grouped into generic force fields, biological force field and class II force fields.[5]They can also be classified as: all atom - parameters provided for every single atom within the system,united atom - parameters provided for all atoms except non-polar hydrogens, coarse grained - an abstract representation of molecules by grouping several atoms into "super-atoms" [33].

For this study 'CVFF' force fields were used based on the findings by Jo Byeongnam, et al [24]. CVFF stands consistent-valence force field. CVFF is developed by Biosym. Biosym merged with Molecular Simulations into the current company Accelrys [34].

The total potential energy of a system is given by the sum of bonded and non-bonded interactions between the particles of the system.

$$Etotal = Ebond + Enon\_bond \quad (2.4)$$

The bonded interaction between the particles of the system Ebond can be further expressed as sum of valence and cross-terms:

$$Etotal = Evalence + Ecrossterm + Enon\_bond \quad (2.5)$$

The bonded valence energy $Evalence$ consists of energy due to stretching of bonds, angle bending between two bonds, twisting (dihedral) and molecules going out of plane (oop).

$$Evalence = Ebond + Eangle + Etorsion + Eoop \quad (2.6)$$

The different cross terms interactions caused by the surrounding atoms are:

- bond-bond: interaction between adjacent bonds
- angle-angle: interaction between angles having common vertex atom;
- bond-angle: interaction between an angle and one of its bond;
- end-bond-torsion: interaction between a dihedral and one of its end bond
- middle-bond-torsion: interaction between a dihedral and its middle bond;
- angle-torsion: interaction between a dihedral and one of its angles;
- angle-angle-torsion: interaction between a dihedral and its two valence angles [31].

Fig. 10 is a pictorial representation of the various interactions due to the bonds between the particles.

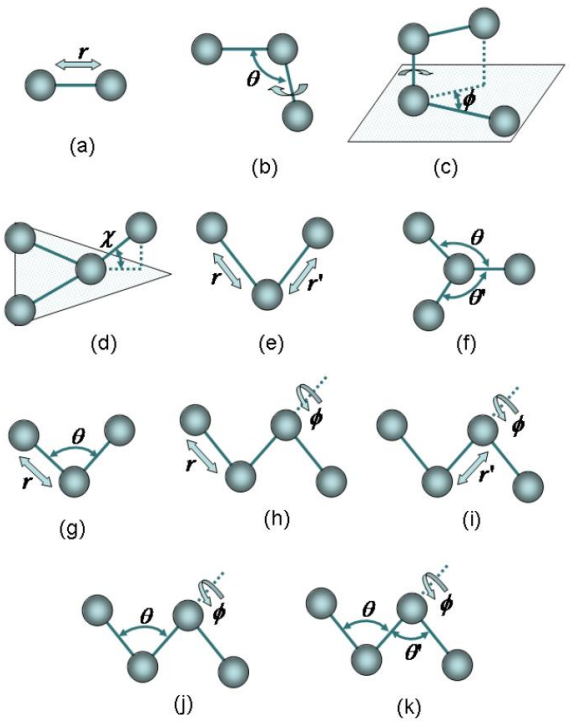

Figure 10 Types of bonded interactions between the particles of a system [31]

The bonded interactions considered for this study are bond-stretching, bending, and torsion and are given by following equation:

$$E_{bond} = K_s * (r - r_0)^2 + K_b * (\theta - \theta_0) + K_t * (1 + d * cos(n\phi)) \quad (2.7)$$

Further, the non-bonded interaction is given by,

$$E_{non\_bonded} = E_{coulumb} + E_{LJ} \quad (2.8)$$

$$E_{non\_bonded} = \frac{q_{i*}q_j}{r} + 4\varepsilon\left[\left(\frac{\sigma}{r}\right)^{12} - \left(\frac{\sigma}{r}\right)^{6}\right] \quad (2.9)$$

In this,

q_i, q_j : partial charges

r : distance between the atoms

σ : Finite distance at which the inter-particle potential is zero

ε: Depth of the potential well.

The LJ potential, E_{ij} stands for Lennard-Jones potential. It's a mathematical model that approximates the interaction between a pair of neutral atoms or molecules. It can also be represented in form:

$$E_{LJ} = \varepsilon\left[\left(\frac{r_m}{r}\right)^{12} - 2\left(\frac{r_m}{r}\right)^{6}\right] \quad (2.10)$$

Where, r_m: distance at which the potential reaches its minimum

In a system with N particles, the numbers of pairwise interactions are N2, which are computationally very costly. To minimize the computation cost, a cut off radius, rc is defined. The atoms or molecules within the cut off distance are only considered for the pairwise interactions as shown in Figure 11.

Mathematically, this can be defined as

$$E_{lj,short\ range} = \begin{cases} V_{lj}(r) - V_{lj}(r_c) & r_{ij} \leq r_c \\ 0 & r_{ij} > r_c \end{cases} \quad (2.11)$$

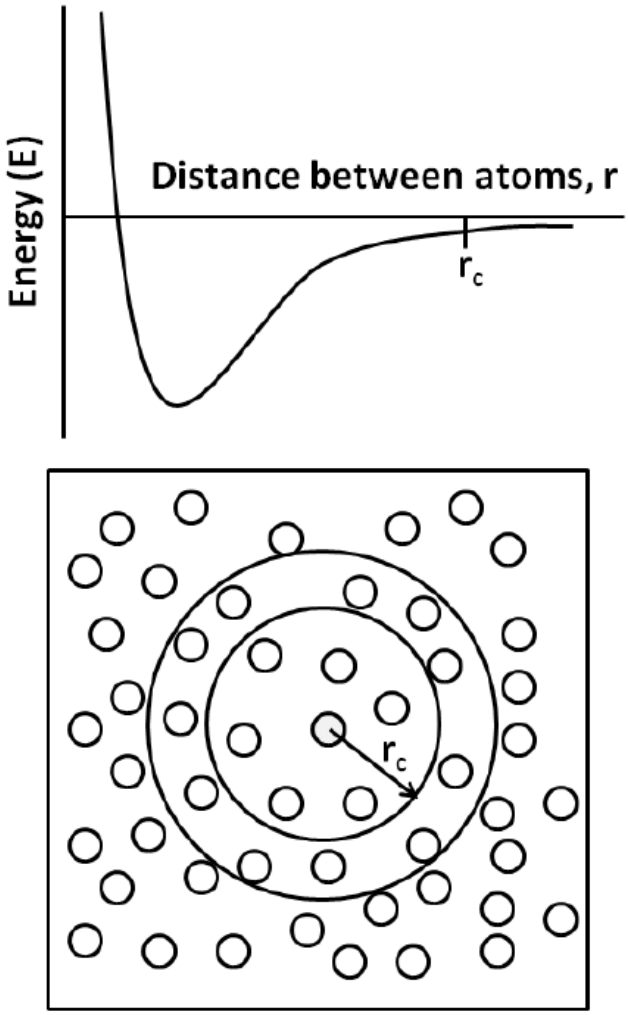

Figure 11 Non-bonded Leonard-Jones potential between two atoms and the use of cut off radius to reduce the computational cost by eliminating calculations between atoms separated by large distance [31]

III. Ensembles:

In physics, the term ensemble refers to a group of similar systems, or different states of the same system. One state of these states represents the system at a particular instant. The probability of occurrence of each state is same. Hence, ensemble is a system having different microscopic states representing particular identical macroscopic or thermodynamics state of the system. As mentioned earlier, Newton's laws of motion form the base of Molecular dynamics simulations. But they consider only constant energy surfaces which is a characteristic of an isolated system. But when real systems are considered, various factors like pressures, external forces and thermal energy exchange are required to be considered. These different macro-scopic factors give rise to different ensembles. The different ensembles are:

- Micro canonical Ensemble (NVE): This thermodynamic state of the system is characterized by constant number of atoms, N, constant volume, V and constant energy E. It corresponds to a thermally isolated system having constant total energy.
- Canonical Ensemble (NVT): This thermodynamic state of the system is characterized by constant number of atoms, N, constant volume, V and constant temperature; T. It is ensemble of systems, which exchange energy with a large heat reservoir. With large heat capacity of the heat reservoir, constant temperature for the coupled system is maintained well.
- Isobaric-Isothermal Ensemble (NPT): This thermodynamic state of the system is characterized by constant number of atoms, N, constant pressure, P and constant temperature; T. It is ensemble of systems, which exchange energy with a large heat reservoir at constant temperature. The volume of systems changes corresponding to the applied external pressure.

Chapter 4

Interfacial Thermal Resistance

Interfacial thermal resistance (i.e. Kapitza resistance) is the resistance to thermal transport (i.e., resistance to heat transfer due to different spectral distribution of molecular vibrations or phonon transport in the different media) that typically occurs at the interface between a solid surface and liquid molecules that are located in the vicinity of the solid surface [34]. Unlike thermal contact resistance it is the thermal transport resistance that occurs due to different rates of phonon propagation in different materials that are in mutual contact. Such resistance exists even when two media are in perfect thermal contact. Hence, Kapitza resistance exists due to the difference in vibrational properties between different materials. It is insignificant and is usually neglected for macroscopic heat transfer. But it plays a significant role for nano-scale heat transfer. With large surface area of nanoparticles, the interfacial area between the surface of the nanoparticle and the surrounding liquid molecules is also very large. This large specific interfacial area significantly increases the effect of the interfacial thermal resistance on the heat transfer within the nanofluid. The interfacial thermal resistance acts as a thermal barrier. If the nanoparticle size decreases, the surface area of the nanoparticle increases and the effect of the interfacial thermal resistance increases, which leads to a decrease of the effective thermal conductivity of the nanofluid [36].

Lumped capacitance

One of the methods to measure Kapitza resistance is the lumped capacitance method. In this method, the system is divided into small lumps and the temperature difference within the lump is assumed negligible. Same approach is considered for the molten salt nanofluid mixture.

Assuming that a nanoparticle in a fluid ("nanofluid") is highly conductive (Biot number « 1), the temperature gradient within the entire nanoparticle will be zero as compared to the surface temperature of the nanoparticle. As mentioned earlier, the interfacial thermal resistance dominates the heat transfer in nanofluids, the total heat transfer between the nanoparticle and the surrounding fluid can be simplified as follows

$$\dot{Q} = \rho_{np} V_{np} C_{np,p} \frac{dT}{dt} \approx \frac{A_s}{R_b} (T_s - T_f) \tag{3.1}$$

Where, t -time, ρ_{np} - density of the nanoparticle, V_{np} -volume of the nanoparticle, $C_{p,np}$ - specific heat capacity of the nanoparticle, A_s - interfacial area of the nanoparticle, R_b - interfacial thermal resistance, T_s - temperature of the nanoparticle, and T_f - temperature of the fluid. Integration of this equation gives:

$$\frac{(T_s - T_f)}{(T_{s,i} - T_f)} = e^{-\frac{A_s}{\rho_{np} V_{np} C_{np,p} R_b} * t} = e^{-\frac{t}{\tau}} \tag{3.2}$$

The time constant, τ is then a function of R_b, and is expressed as:

$$\tau = \frac{\rho_{np} V_{np} C_{np,p} R_b}{A_s} \tag{3.3}$$

Interfacial thermal resistance is a difficult property to measure experimentally. The best method to measure and analyze this property is by computational analysis based on lumped capacitance method. The temperatures changes of the silica surface and the surrounding molten salt is measured to calculate the time constant. Using equation (2.13) the kapitza resistance is measured.

There are just approximate values available for interfacial thermal resistance in case of nanofluids to check the accuracy of the values obtained. Hence, for validating the obtained value, comparative study is the best approach. For this purpose, literature survey gave few set of values done for similar kind of studies.

Table 3 Interfacial thermal resistance values for various Nanocomposites /nanofluid mixtures.

Nanocomposites/Nanofluid mixtures	Interfacial Thermal Resistancee
Alumina nanofluids (37)	2.0e-8 m2k/W
Water-in-FC72 nanofluids(38)	1.5e-8 m2k/W
Amorphous SiO2(39)	3.84e-9 m2k/W
Crystalline SiO2(39)	1.71e-9 m2k/W
Si/Ag interface(40)	4.9e-9 m2k/W
SWCNT-Water (41)	1.22e-7m2k/W
CNT/octane molecule(42)	4e-8m2k/W

Chapter 5

Methodology

Selection of software package for simulation for a particular application is one of the important tasks as it affects the computational cost, time of simulation, accuracy, ease of simulation and availability. There are many types of softwares available in the market, some of which are: AMBER, CHARMM, GROMACS, LAMMPS, Material Studio, NAMD+VMD etc. For this study and application, we choose the LAMMPS software [9, 10]. To create the starting structure with the salts and the amorphous silica nano crystal structure, Material Studio was used. Also, to visualize the simulation at intermediate steps for validating the simulation, VMD was used.

LAMMPS

LAMMPS stands for Large-scale Atomic/Molecular Massively Parallel Simulator. LAMMPS is classical open source molecular dynamics simulation software originally developed under a US Department of Energy CRADA (Cooperative Research and Development Agreement) between two DOE labs and 3 companies. It is distributed by Sandia National Labs. It was originally written in FORTRAN and later converted to C++ for ease of use. It uses message passing interface (MPI) protocol and is designed to run efficiently on parallel computers. It can model solid, liquid or gaseous systems. It can model atomic, polymeric, biological, metallic, granular, and coarse-grained systems using a variety of force fields and boundary conditions.

A general script for running simulations in LAMMPS includes following steps:

Initialization: In this section, terms like units, dimensions, boundary types like periodic etc. are defined.

Defining Simulation Box: In this section, details about the simulation box like box size, atom types, pair styles, bonding, angle, dihedral, improper styles, etc. are given to replicate the actual system as true as possible.

The above two step in combined are sometimes termed as Problem Setup.

Selection of settings: This is one the most important section while making scripts for simulation. The parameters selected in this section define the conditions in which the system needs to simulate like velocities, temperature, pressures, etc. It is also sometimes termed as Minimization and/or Equilibration Run.

Calculations and Outputs: As the name defines, in this section parameters for calculating required outputs are defined. They could be anything from simple variables to complex equations. Examples can be energy values, density equations etc. Outputs can be either obtained in various ways like numerical values, visual data etc. according to the requirement of analysis. This is also sometimes called as the Production Run.

Material Studio

Materials Studio is a complete modeling and simulation software developed and distributed by Accelrys. It is designed to allow researchers in materials science and chemistry to predict and understand the relationships of a material's atomic and molecular structure with its properties and behavior. Materials Studio includes a graphical user environment—Materials Studio Visualizer— in which researchers can construct, manipulate and view models of molecules, crystalline materials, surfaces, polymers, and mesoscale structures[43].

Chapter 6

Model and Simulations Details

Problem Setup

The very first step in the simulation is to make the starting structure of the system. For this study, the simulation box with CO3 molecules and Li+ and K+ ions was made in the proportion of 62:38[12] in Material Studio package(Box size 47*47*47 A)(Fig 13). Further amorphous spherical silica nanostructure was made using amorphous builder module of Material studio (Fig.14). The size was selected such that it accounted to 1% in the mixture. This was placed such that the center of the nanostructure coincides with the center of the simulation box. Few modifications were done to get a neutrally charged system. Fig.15 shows a typical starting structure. These files were exported and converted for LAMMPS compatibility using the converting tools available with LAMMPS package. This file acts as the starting input structure for LAMMPS.

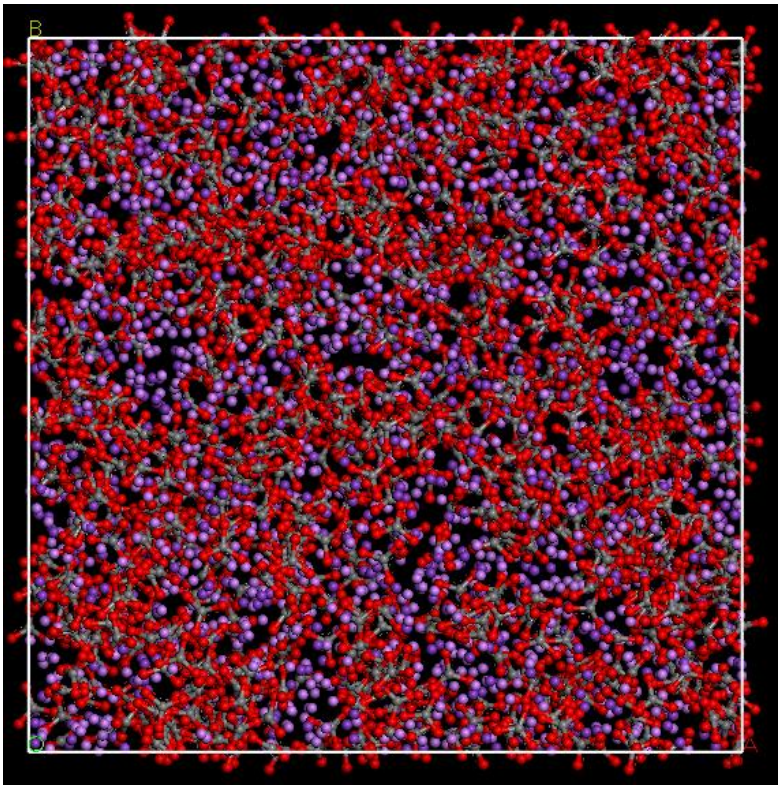

Figure 12 Li2CO3-K2CO3 (62:38) in material studio

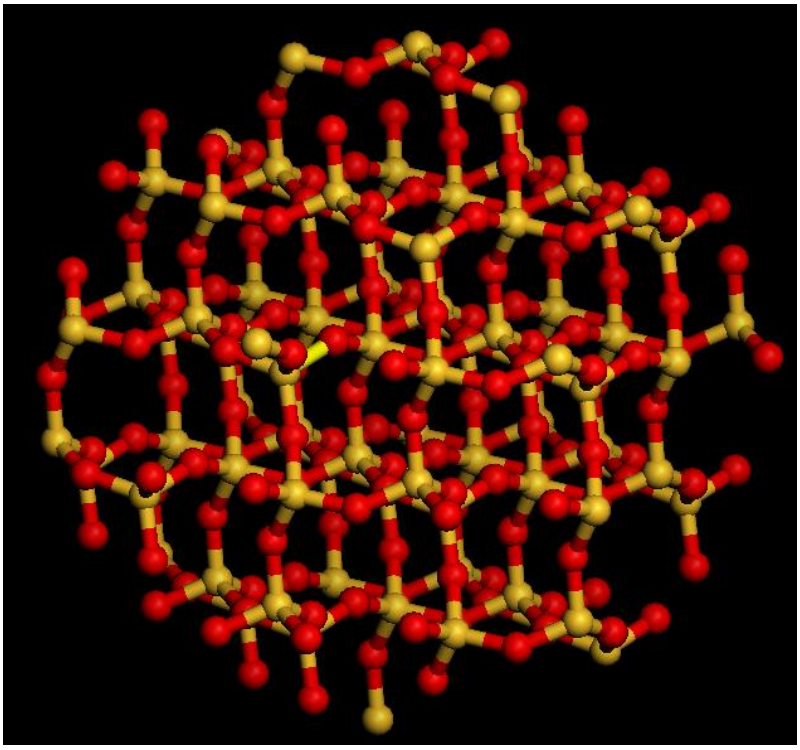

Figure 13 Nanocluster built from alpha quartz crystal

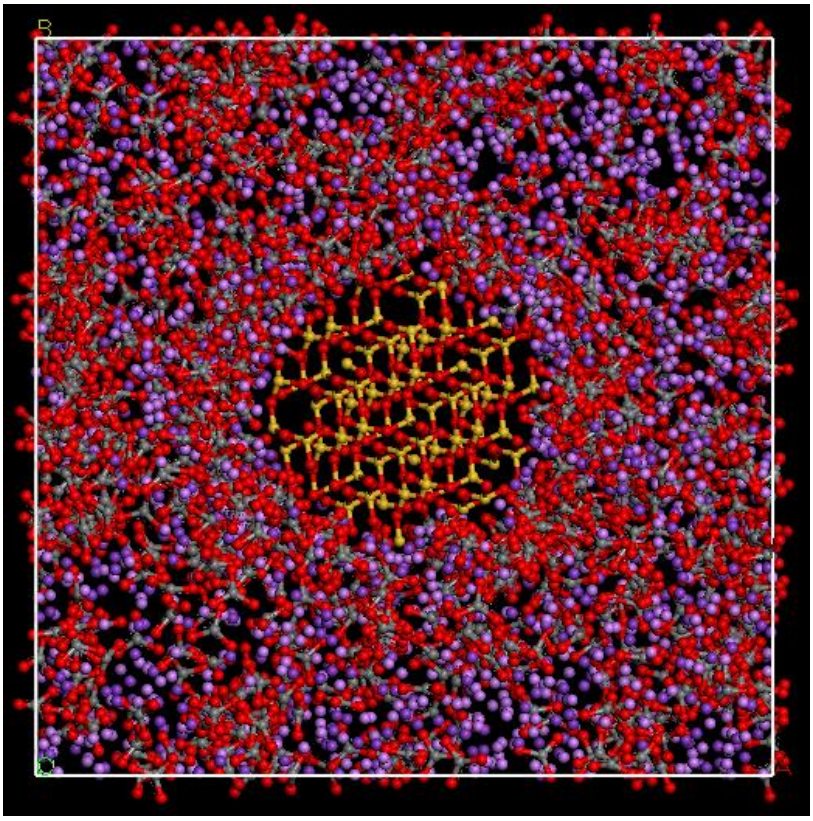

Figure 14 Typical starting structures after placing silica manually at the center of pure carbonate system

Force Fields Parameters

This system was first testing using LJ parameters for Carbonate previously reported by Jo and Banerjee [7] but with Silica to repeat and compare the results for carbonate salts with silica against carbonate salts with CNT. The Silica parameters were taken from [44-45].

Table 4 LJ parameters for Li2CO3-K2CO3/SiO2

Interactions	ε(kcal/mol)	σ[A]	Charge
C-C	0.055	3.617	1.54
O-O	0.228	2.88	-1.18
Li-Li	4.735	2.839	+1.00
K-K	5.451	3.197	+1.00
Si-Si	0.04002	4.05324	0.30
O-O	0.228	2.8598	-0.15

Simulations

- Pre-equilibration Run (pre-NVE)

The silica nanocluster is manually placed at the center of the pure eutectic simulation box. Because of this there is possibility of large vacuum around the silica making a unstable starting structure. Hence, the system is first given a NVE run, letting its temperature change but maintaining the volume. After this run, it is expected the vacuum space is then taken by the ions making a uniform designed structure

- Minimization Run

As mentioned earlier, the starting structure is made by randomly placing the molecules inside the simulation box. Also the Silica nanostructure is manually placed approximately at the center. Even after a pre-NVE, the atoms of the matrix molecules are can still be poorly placed or can also be overlapping with atoms of silica nanostructures. If simulations are performed with this structure, very large forces can act on the atoms, resulting very high velocities to the atoms. This might or will lead to high computational instabilities. To avoid this instability, potential energy of the system, bonded and non-bonded energy, is minimized before running the dynamics. This is called Minimization. A point to be noted is that the kinetic energy of the system is not considered during minimization. LAMMPS uses Polak-Ribiere version of the conjugate gradient (CG)

algorithm to minimize the energy [12]. In this study the minimizations is done in two steps. For the first minimization, the silica nanostructure is fixed at its place and energy of the surrounding matrix molecules is minimized. This is done because of short and uncertain distances between them and silica, the surrounding ions can tend to distort the silica structure. Hence, fixing the silica and minimizing the surrounding atoms will help getting a better structure. In second minimization, the silica nanostructure is 'unfreeze' or relaxed and the whole system is allowed to minimize. The minimization step helps in achieving a good initialized system structure.

- Equilibration Run

Minimization is followed by equilibration. Theoretically, the system is at 0K after minimization. To start the simulation dynamics the system has to be brought to base temperature of interest. For this study it is 800K. Here simulation is performed in a NVE ensemble with time step of 50ps with random velocities assigned to the atoms at 800K. During this relaxation some of the kinetic energy is converted to potential energy due the non-equilibrium initial configuration (coordinates). Hence the final temperature of the system is lower than 800K. In NVE ensemble, the final temperature converges to a value close to 600K.

- Production Run

After the NVE the temperatures of the system is raised only till 600K. To raise the temperature further, the system is than run under NPT giving temperature of 800K. In this simulation, density values are calculated for studying the concentration gradients and composition changes at the interface of nanocluster and salts. Also, production runs at NVE for calculating the interfacial thermal resistance. The system is run giving a temperature of 1400K to the silica nanocluster. The temperature difference over a time period gives the value for Kapitza resistance.

Chapter 7

Results and Discussions

Parameter improvisation

As mentioned in the objectives, the system was first tested using the parameters already published. Using the position of the atoms from the silica surface, density plots were made. Fig 16 shows the density plots. The average value of density obtained was 1.56 kg/cm3 as compared to the 1.9790825 kg/cm3 literature value for pure Li2CO3-K2CO3.

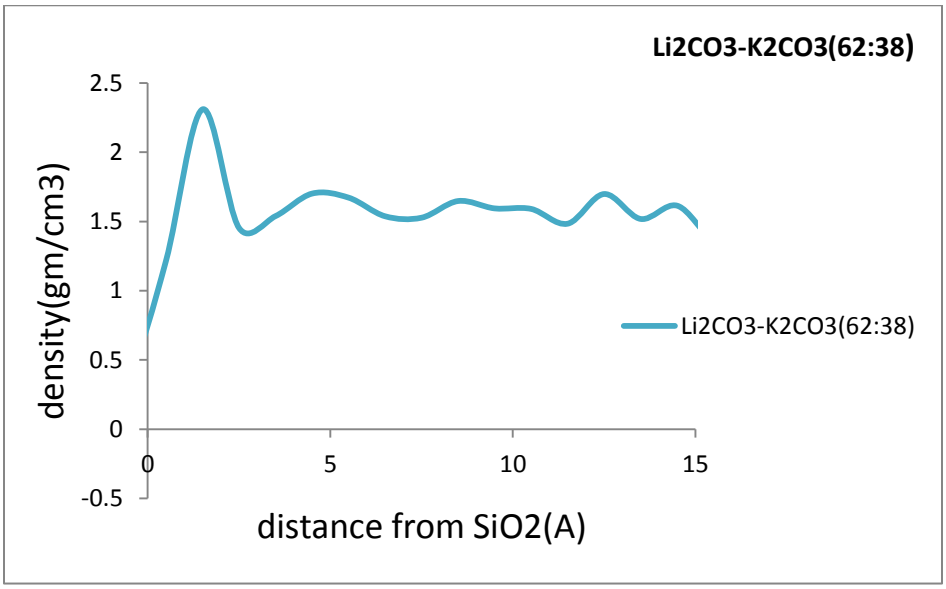

Figure 15 Density plots for Li2CO3-K2CO3/SiO2 using parameters from table 2

To reduce these errors, new parameter combinations were used. Table 5 gives the new parameters.

Table 5 Improved LJ parameters to reduce the errors [46-47]

Interactions	ε(kcal/mol)	σ[A]	Charge
C-C	0.148	3.617	1.54
O-O	0.228	2.88	-1.18
Li-Li	0.149	2.37	+1.00
K-K	0.100	3.0469	+1.00
Si-Si	0.300	3.827	+0.90
O-O	0.150	3.11814	-0.45

The plots obtained with these new simulations showed an improvement in the density value. The new density value obtained came out to be 2.131 kg/cm3 as compared to the previous 1.56 kg/cm3. Fig. 17 shows the plots for the same.

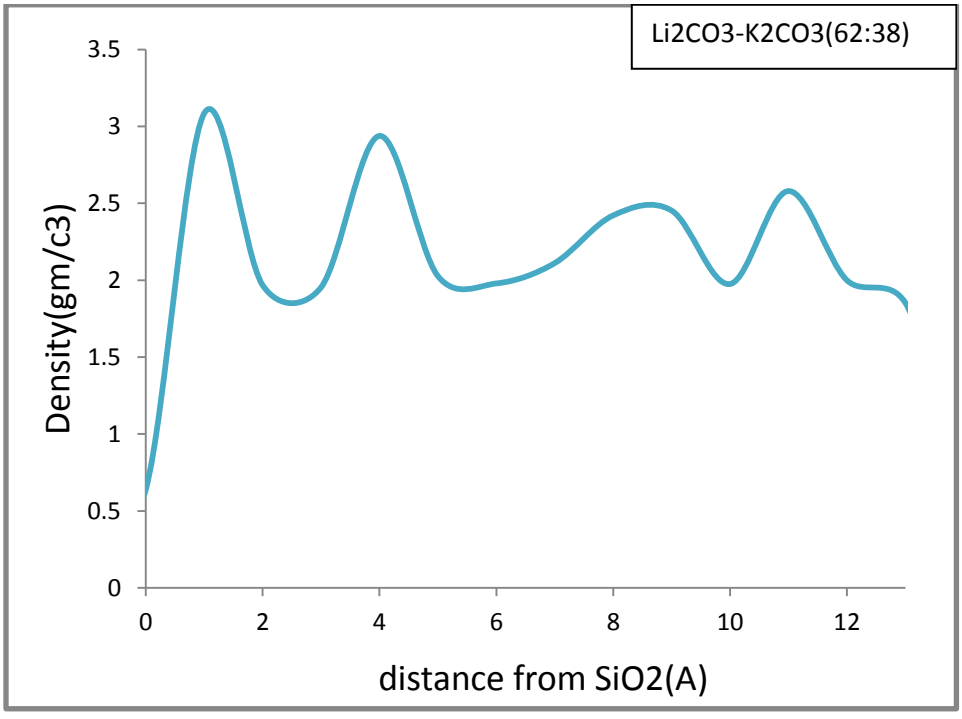

Figure 16 Density plots for Li2CO3-K2CO3/SiO2 using parameters from table

Compressed Layer

Further analysis was done to find density variations around the nanostructures. For this again, the same density plots were used. Fig.17 shows that there are two peaks seen near the nanostructure, from which existence of dense layers around the silica can be inferred. Similar results have been published [48] to support existence of dense layers supporting the formation of nanostrutcures.This is formed due to electrostatic attractions between the K+ and Li+ ions and the surface charge of Silica.

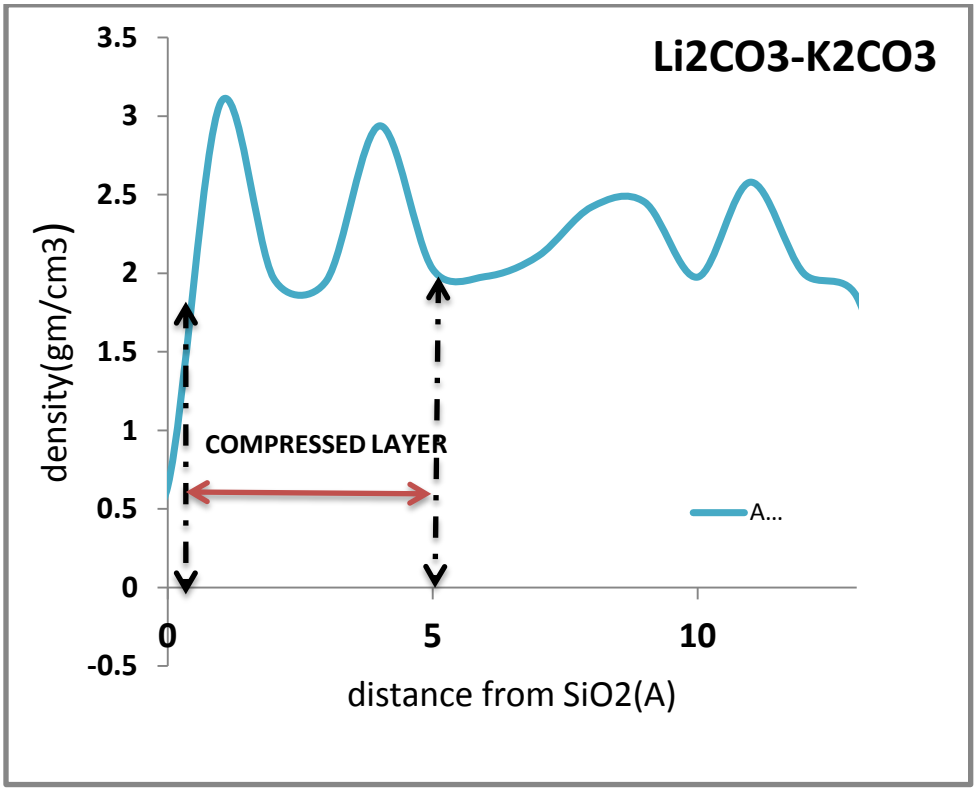

Figure 17 Density simulations to show existence of compressed layers around silica nanostructures.

Liquid Layer Separation

After getting results to support the existence of a dense layer around the silica, analysis was further carried out to study the composition changes around the silica with aim of finding the cause of formation of nanostructures. For finding this, the behavior of Li+ and K+ ions around the silica was required to be studied for studying the phase changes. For this purpose, the positions of the Li+ and K+ ions was plotted from the Silica surface in Z direction as shown if Fig 18.

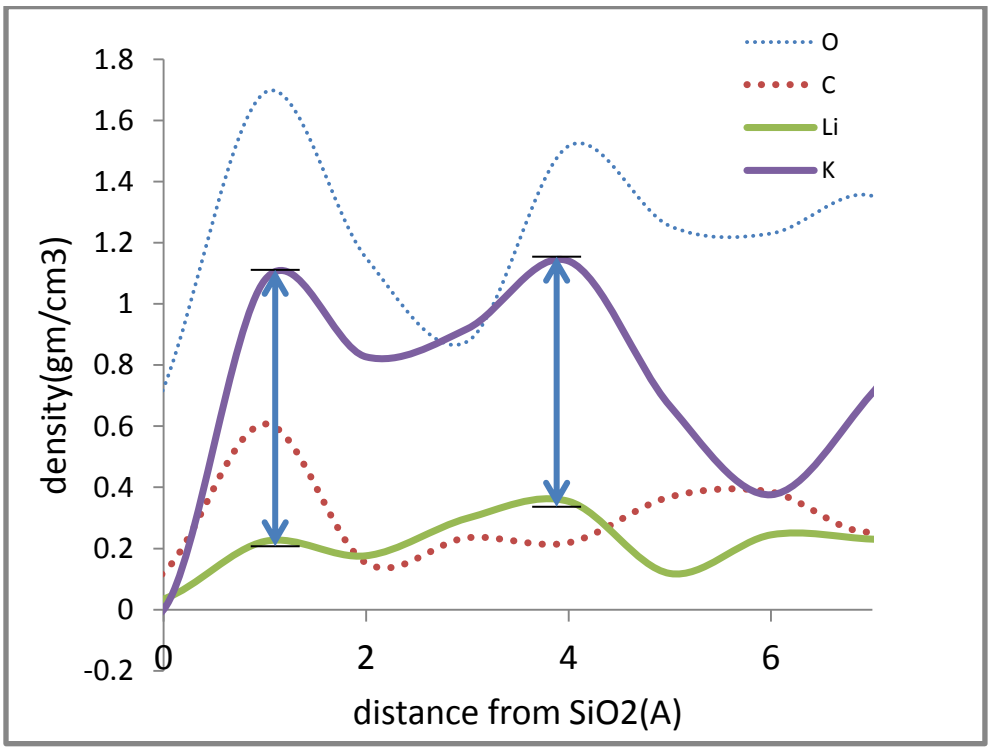

Figure 18 Liquid layer separations around the Silica

From the plot, it is seen that the concentration of K+ ions around silica is more as compared to Li+ ions. The difference in the density shows nothing but the separation of the two ions around the silica.

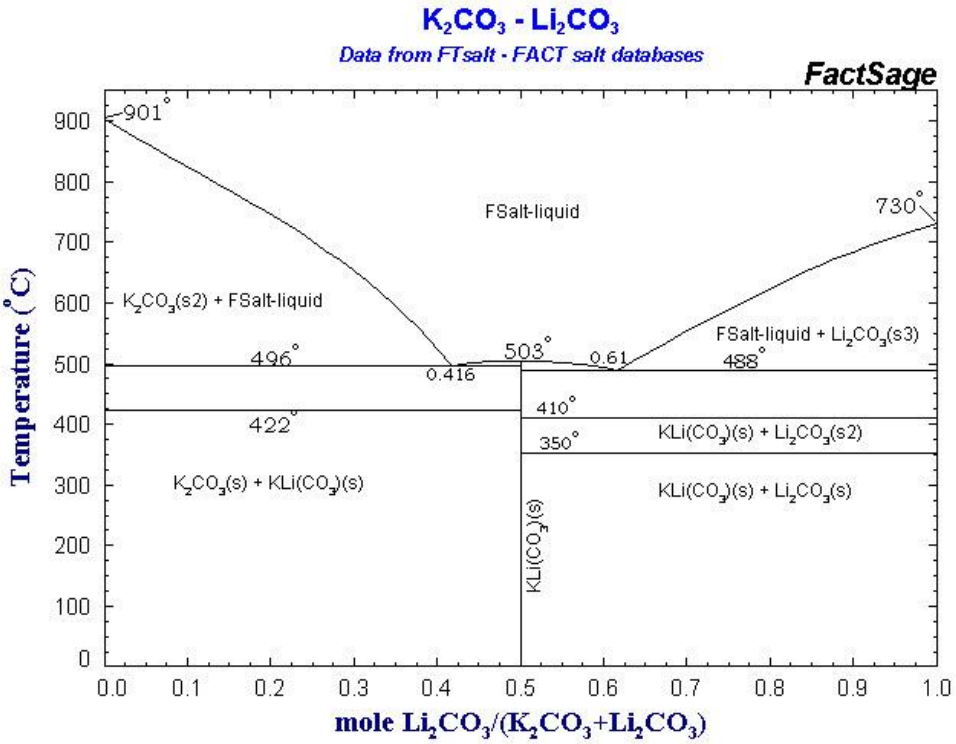

Figure 19 Phase Diagram for Li2CO3-K2CO3 eutectic.

If we compare the starting composition of Li2CO3-K2CO3 (62:38) with the concentration seen the liquid layer separation, it can be said that this composition is completely changed. This phenomenon can be explained with the help of the phase diagram for Li2CO3-K2CO3 eutectic. So it can be said that the attraction of K+ ions and silica is more than Li+. Due to the changes in the concentration, the K+ ions crystalizes before Li+, getting attached to Silica and giving birth to formation of nanostructures

Interfacial thermal resistance value for SiO2/Li2CO3-K2CO3 interface

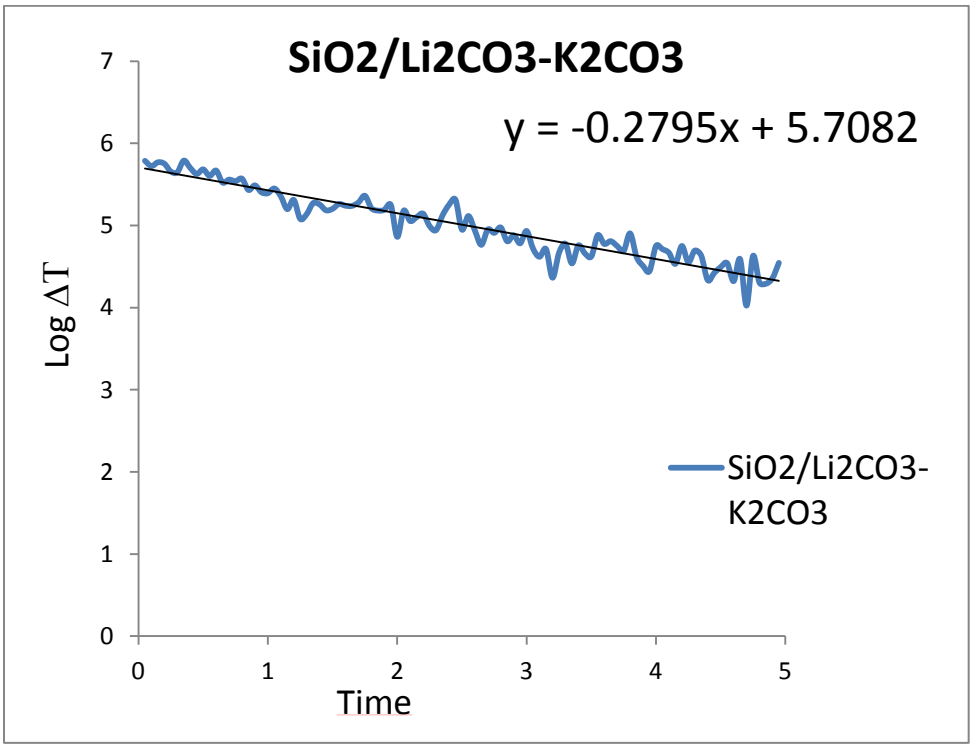

Figure 20 Interfacial thermal resistances for Li2CO3-K2CO3/SiO2 interface

To measure the kapitza resistance value the log of temperature difference against time was plotted. The negative inverse of slope gave the Kapitza resistance value from equations (3.1), (3.2) and (3.3). The values obtained were comparable to the reported values.

Table 6 Interfacial thermal resistance value

as compared to other published values for different nanofluids.

Salt	Rb , m2K/W
SiO2/Li2CO3-K2CO3	6.38896e-09
Amorphous SiO2	3.84e-9
Crystalline SiO2	1.71e-9
Si/Ag interface	4.9e-9

Chapter 8

Conclusions and Future Work

- Parameters and results reported by Jo and Banerjee [9] were wrong as they gave less average density values for carbonate salts as compared to the literature values. Better parameters were required to be used to reduce this error.
- Better force-field parameters were hence found reducing the error and improving the values for density from 1.56kg/cm3 to 2.31kg/cm3.
- Compressed layers with peak heights around the silica nanocluster are seen in density simulations. This support the existence of dense layer around the nanostructures as seen in the back scattered images of Li2CO3-K2CO3/SiO2 by Tiznobaik et al (12).
- The difference in ionic concentration ratio near nano-structure support the claim of existence of electrostatic forces of attractions giving birth to formation of nano-structures with proximity of potassium ions.
- Interfacial thermal resistance exists at the SiO2 and Li2CO3-K2CO3 interface. It can be crucial at nano-scale and hence should not be neglected for thermal analysis.

A lot of experiments are in progress testing different binary, ternary and even quaternary salts of Nitrates, Carbonates, and Chlorides etc. with various nanomaterials like Silica, CNT etc. Future studies would comprise of simulating various such kinds of salts. Simulations would also include calculating various thermo-physical properties ofsuch nano-fluids.

References

1) Solangi, K. H., et al. "A review on global solar energy policy." Renewable and Sustainable Energy Reviews 15.4 (2011): 2149-2163
2) Hasnain SMA SH, Elani UA. Solar energy education – a viable pathway for sustainable development 1998; 14(1–4):387–92.
3) Bourdiros EL. Renewable energy sources education and research as an education for survival.Progress in solar energy education, vol.1. Borlange, Sweden;1991. p. 12–16.
4) ChartersSWW.Solar energy educational pathways. Proceedings of 2nd World Renewable Energy Congress. (Reading, UK); 1992.
5) Garg P, Kandpa TC. Renewable energy education in developing countries. Proceedings of 2nd world renewable energy congress. (Reading, UK); 1992.
6) Hasnain SM, Elani UA, Alawaji SH, Abaoud HA, Smiai MS. Prospects and proposals for solar energy education programs. Appl Energy 1995;52:307–14
7) P. E. Glaser, \Power from the Sun: its future," Science, vol. 162, pp. 857{861, 1968.
8) B. C. Staley, J. Goodward, C. Rigdon, and A. MacBride, \Juice From Concentrate: Reducing Emissions with Concentrating Solar Thermal Power," world resources institute, May 2009
9) “Block diagram of csp." [Online]. Available: http://www.volkerquaschning. de/articles/fundamentals2/index.php
10) Dudda, Bharath, and Donghyun Shin, "Effect of nanoparticle dispersion on specific heat capacity of a binary nitrate salt eutectic for concentrated solar power applications." *International Journal of Thermal Sciences* 69 (2013): 37-42
11) R. Palgrave, Innovation in CSP, Renew. Energy Focus 9 (6) (2008) 44–49

12) Tiznobaik, Hani, and Donghyun Shin, "Enhanced specific heat capacity of high temperature molten salt-based nanofluids." *International Journal of Heat and Mass Transfer* 57.2 (2013): 542-548

13) National Renewable Energy Laboratory, jan 2010. [Online]. Available: http://www.nrel.gov/csp/troughnet/thermal energy storage.html

14) B. Kelly and D. Kearney, “Thermal storage commercial plant design study for a 2-tank indirect molten salt system,” 2006

15) R. E. Project, “Andasol-1 thermo solar energy.” [Online]. Available: http://www.estelasolar.eu/_leadmin/ESTELAdocs/documents/powerplants/Andaol.pdf

16) R. Palgrave, Innovation in CSP, Renew. Energy Focus 9 (6) (2008) 44–49

17) G. Janz, C. Allen, N. Bansal, R. Murphy, R. Tomkins, Physical properties data compilations relevant to energy storage, US Dept. of Commerce, National Bureau of Standards, Washington, DC, 1979.

18) N. Araki, M. Matsuura, A. Makino, T. Hirata, Y. Kato, Measurement of thermophysical properties of molten salts: mixtures of alkaline carbonate salts, Int. J. Thermophys. 9 (2005) 1071–1080

19) S. Choi, Enhancing thermal conductivity of fluids with nanoparticles, in: D.A. Siginer, H.P. Wang (Eds.), Developments and Applications of Non-Newtonian Flows, ASME, 1995, pp. 99–105. FED-231/MD-66.

20) Y. Xuan, Q. Li, Heat transfer enhancement of nanofluids, Int. J. Heat Fluid Flow 21 (2000) 58–64.

21) S. Lee, S.U.S. Choi, S. Li, J.A. Eastman, Measuring thermal conductivity of fluids containing oxide nanoparticles, ASME J. Heat Transfer 121 (1999) 280–289.

22) S.K. Das, N. Putta, P. Thiesen, W. Roetzel, Temperature dependence of thermal conductivity enhancement for nanofluids, ASME Trans. J. Heat Transfer 125 (2003) 567–574.

23) J.A. Eastman, S.U.S. Choi, S. Li, W. Yu, L.J. Thompson, Anomalously increased effective thermal conductivities of ethylene glycol-based nanofluids containing copper nanoparticles, Appl. Phys. Lett. 78 (6) (2001) 718–720

24) Jo Byeongnam, Banerjee Debjyoti; “Effect of Dispersion Homogeneity on Specific Heat Capacity Enhancement of Molten Salt Nanomaterials Using Carbon Nanotubes”, *J. Sol. Energy Eng. 137, 011011 (2014) (9 pages)*

25) Dudda, Bharath, and Donghyun Shin. "Effect of nanoparticle dispersion on specific heat capacity of a binary nitrate salt eutectic for concentrated solar power applications." *International Journal of Thermal Sciences* 69 (2013): 37-42.

26) Shin, D., and Banerjee, D, 2011, “Enhanced Specific Heat of SiO2 Nanofluid,”Journal of Heat Transfer, 133(2), pp. 024501

27) Shin, D., and Banerjee, D, 2011, “Enhancement of Specific Heat Capacity of High- Temperature Silica-Nanofluids Synthesized in Alkali Chloride Salt Eutectics for Solar Thermal-Energy Storage Applications,” International Journal of Heat and Mass Transfer, 54(5-6), pp. 1064-1070

28) Andreu-Cabedo, Patricia, et al. "Increment of specific heat capacity of solar salt with SiO2 nanoparticles." *Nanoscale research letters* 9.1 (2014): 1-11

29) Tiznobaik, Hani, and Donghyun Shin. "Experimental validation of enhanced heat capacity of ionic liquid-based nanomaterial." *Applied Physics Letters*102.17 (2013): 173906

30) http://en.wikipedia.org/wiki/Computer_simulation#mediaviewer/File:Molecular_simulation_process.svg

31) Singh Navdeep, *Computational analysis of thermo-fluidic characteristics of a carbon nano-fin*. Diss. Texas A&M University, 2010

32) D.W. Brenner, *“The art and science of an analytic potential," Computer Simulation of Materials at Atomic Level, vol. 217, pp. 23-40, 2000*

33) http://www.gromacs.org/Documentation/Terminology/Force_Fields

34) Accelrys, “http:www.accelrys.com/about/," 2008

35) Swartz, E.T., and Pohl, R.O., 1989, "Thermal Boundary Resistance," Rev. Mod.Phys., 61, pp. 605–668

36) Shin, Donghyun. *Molten salt nanomaterials for thermal energy storage and concentrated solar power applications*. Diss. Ph. D. thesis, Texas A&M University, College Station, TX, 2011

37) Kim, Seokwon, et al. "Rheological properties of alumina nanofluids and their implication to the heat transfer enhancement mechanism." *Journal of Applied Physics* 110.3 (2011): 034316

38) Han, Zenghu. "Nanofluids with enhanced thermal transport properties." (2008).

39) *Kapitza conductance of silicon–amorphous polyethylene interfaces by moleculardynamics simulations*

40) Termentzidis, Konstantinos, et al. "Thermal conductivity and thermal boundary resistance of nanostructures." *Nanoscale research letters* 6.1 (2011): 1-10.

41) Huxtable, Scott T., et al. "Interfacial heat flow in carbon nanotube suspensions." *Nature materials* 2.11 (2003): 731-734

42) Shenogin, S., Xue, L., Ozisik, R., Keblinski, P., and Cahill, D.G., 2004, “Role of hermal Boundary Resistance on The Heat Flow in Carbon-Nanotube Composites,” Journal of Applied Physics, 95(12), pp. 8136–8144

43) Accelrys, http://accelrys.com/products/materials-studio/

44) Hill, Joerg R., and Joachim Sauer. "Molecular mechanics potential for silica and zeolite catalysts based on ab initio calculations. 1. Dense and microporous silica." *The Journal of Physical Chemistry* 98.4 (1994): 1238-1244.

45) Jung, Seunghwan. *Numerical and experimental investigation of inorganic nanomaterials for thermal energy storage (tes) and concentrated solar power (csp) applications*. Texas A&M University, 2012.

46) Cruz-Chu, Eduardo R., Aleksei Aksimentiev, and Klaus Schulten. "Water-silica force field for simulating nanodevices." *The Journal of Physical Chemistry B*110.43 (2006): 21497-21508.

47) Averina, M. I., A. V. Egorov, and V. I. Chizhik. "Solvation of cations in the LiNO3-Ca (NO3) 2-H2O system at 25° C. A molecular dynamics simulation study." *Russian Journal of Physical Chemistry A* 88.8 (2014): 1340-1344.

48) Cicero, Giancarlo, et al. "Water confined in nanotubes and between graphene sheets: A first principle study." *Journal of the American Chemical Society*130.6 (2008): 1871-1878

49) M.P. Allen and D.J. Tildesley, Computer simulation of liquids, Clarendon Press,Oxford, 1987

Biographical Information

Vidula Pawar is a graduate student at the Mechanical Engineering department of The University of Texas at Arlington. She completed her Masters of Sciences degree requirement by defending her thesis on the topic ‘Computational analysis of nanostructures formed in molten salt nanofluids in Fall 2014. She holds a Bachelors of Engineering degree in Mechanical Engineering from Univeristy of Pune, India. Her interests are Nanotechnology, thermal analysis, design, automation and robotics